

STATIC AND DYNAMIC STRUCTURAL MONITORING OF CIVIL INFRASTRUCTURE OBJECTS WITH GNSS

CAROLINE SCHÖNBERGER^{*}, WERNER LIENHART^{*} AND BENJAMIN KADEN[†]

^{*} IGMS - Institute of Engineering Geodesy and Measurement Systems

Graz University of Technology

Steyrergasse 30

8010 Graz, Austria

e-mail: c.schoenberger@tugraz.at, werner.lienhart@tugraz.at, <https://www.igms.tugraz.at>

[†] Verbund Hydro Power GmbH

Europaplatz 2

1150 Vienna, Austria

email: benjamin.kaden@verbund.com

Abstract. Continuous monitoring of civil structures, especially critical infrastructure, is important to ensure a safe operation and to enable condition-based maintenance. For a complete assessment of the structure's performance its static and dynamic behaviour have to be observed. Traditionally, different types of sensors are used to fulfil this task, e.g. accelerometers for the measurement of vibrations and geodetic sensors for static monitoring.

This paper focusses on a new approach where Global Navigation Satellite System (GNSS) receivers are used to monitor slow as well as dynamic movements. Although the absolute accuracy of GNSS real time kinematic (RTK) solutions is in the centimetre range, vibrations with amplitudes in the millimetre range can be identified in the frequency spectrum since long wavelength effects cancel out when deriving accelerations.

In order to assess the frequency and amplitude resolution, dynamic GNSS measurements were carried out at the rooftop laboratory, with the GNSS antenna mounted on a shaking table. Data was collected with up to 20Hz and the vibrations of the antenna were modified in amplitude as well as in frequency. We discuss the dependency on the measurement frequency of the reference station and demonstrate the great possibilities of modern GNSS receivers.

The performance of the proposed monitoring approach was also verified in field campaigns, where six GNSS receivers were mounted on the highest water dam in Austria. We discuss the right GNSS sensor placement as well as the optimum data recording settings to measure the reaction of the water dam to water level and temperature changes. Furthermore, the occurring motion of the concrete dam during two 1-month measuring periods in spring and autumn is analysed. Finally, the benefits of the combining several GNSS systems (GPS, Galileo and GLONASS) are discussed. Especially at difficult locations like the abutments of the water dam where the nearby mountain slopes cause signal obstructions and significant multipath effects, the use of multiple constellations increase the number of phased-fixed solutions and improves the precision of the determined 3D coordinates.

Key words: GNSS, SHM, Structural Health Monitoring, water dam, critical infrastructure, Galileo, dynamic monitoring

1 INTRODUCTION

Structural monitoring of civil infrastructure is necessary for its safe operation. Therefore, its behaviour to external input, such as wind or temperature has to be observed to detect any abnormal changes. Monitoring is normally done with a combination of different sensors, e.g. total stations or Global Navigation Satellite System (GNSS) receivers for its static displacement and accelerometers for its dynamic response. Advances in GNSS monitoring enables the recording of dynamic responses too [1]. In recent years dynamic GNSS monitoring of bridges [2], towers [3] and buildings [4] was carried out, with recorded eigenfrequencies below 5Hz and displacements of 10-20mm.

Using only one sensor for static and dynamic monitoring leads to many advantages, such as no time synchronisation between different sensors or no coordinate transformation to the same coordinate system are required. Further advantages are less equipment and cables as well as less energy consumption at the monitoring site. Those advantages are topped with GNSS sensors, where a precise time and direct 3D measurements of displacement in a global coordinate system is already provided. Additionally, measurements can be carried out in real time, are weather independent and no line of sight between monitoring points is necessary. On the other hand, limitations of accuracy are multipath errors, bad satellite geometry and low sampling rates [5].

Since the early 1980s the American Global Positioning System (GPS) is available to civil users. In the last decades the Russian Global Navigation Satellite System (GLONASS) and recently the European Galileo system became additional systems. As a result, there is an increasing number of satellites and a better satellite geometry for GNSS observations available.

For deriving the dynamic characteristics of a data time series, a transformation into the frequency domain is needed. Potential approaches are Wavelet Analysis, Fast Fourier Transformation (FFT) or Short Time Fourier Transformation (STFT).

Frequencies smaller than half of the data rate can be derived due to the Nyquist–Shannon sampling theorem [6], where frequencies above this value cause aliasing effects, if they are not filtered.

For the experiments described in this paper, GNSS receivers with a data rate of 20Hz and the three satellite systems, GPS, GLONASS and Galileo are used for two different scenarios. The first one is an experiment on the rooftop laboratory at Graz University of Technology (TU Graz) on a shaking table with controlled oscillations to show the suitability of high rate GNSS for structural monitoring. Therefore, the behavior of amplitude, frequency and noise is studied. The second scenario is a permanent measurement campaign at the highest water dam in Austria, Kölnbreinsperre, to record a long time series with static displacement due to water level rise and temperature changes and the possibility of dynamic events, such as earthquakes or rockslides. The observed displacements are compared to reference measurements by Verbund, the operating company of the water dam.

2 LABORATORY - SHAKING TABLE

The experiment took place at the rooftop laboratory at TU Graz, with very few obstacles to the sky. A Leica GS18 receiver was set up as a reference station on a stable pillar. A Leica

GR30 receiver with an AS10 antenna was used as rover and placed on an APS 400 shaker (Figure 1). This shaker is able to generate controlled oscillations and can be operated in a vertical or horizontal setup. Oscillation from 0.5 to 10Hz with accelerations from 0.3 to 16m/s² were generated in 3 days of testing. The receiver recorded GPS, GLONASS and Galileo signals with a data rate of 20Hz (0.05s).



Figure 1: Experiment setup at the rooftop laboratory. Monitoring site with shaker (vertical: left & horizontal: middle), reference station (right); As a reference a Laser Triangulation Sensor (LTS) was installed.

The data processing chain is shown in Figure 2. The RINEX data of the reference and the rover were processed in postprocessing mode with RTKLIB 2.4.3 [7] and Leica Infinity 2.4.1 using broadcast ephemeris. Afterwards a coordinate transformation into the local Gauß-Krüger (GK) system is performed. On those results an outlier detection using a moving median method and a high-pass Butterworth filter with an edge frequency of 0.5Hz were applied to exclude the impact of long-term effects [8]. To transfer the data into the frequency domain a Fast Fourier Transformation (FFT) and a Short Time Fourier Transform (STFT) were carried out. Furthermore, GNSS data was compared to measurements of a Micro Epsilon optoNCDT 1700-50 laser triangulation sensor (LTS), with a data rate of 312.5Hz and a measurement precision of 3μm [9].

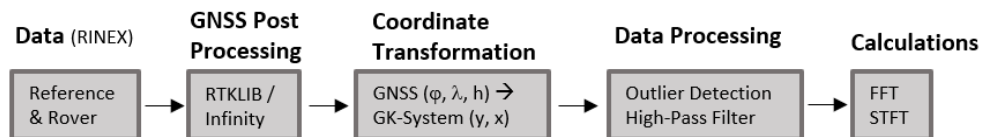


Figure 2: GNSS data processing chain

2.1 Noise and data rate

During this experiment a few minutes of no motion were recorded to study the impact of different satellite systems used for GNSS processing, the behaviour of noise and the influence of the reference data rate.

With the programs RTKLIB and Leica Infinity, the RINEX data was processed with all seven combinations of GPS (G), GLONASS (R) and Galileo (E). The results were compared by their standard deviations (STD) of the no motion time series for all three coordinates, after the high pass filter was applied, Figure 3, left. As expected, the noise is higher for the height component, than in 2D. The combination of GRE leads to the lowest noise with less than 1mm, in all 3 coordinates. Both software packages lead, based on the same data, to different

results. The normally distributed noise for the height (GRE) processed in Infinity and RTKLIB is shown in a histogram in Figure 3, right, with a mean value of 0 and a STD of 1.9mm for the data processing in Infinity and 0.9mm for the data processing in RTKLIB.

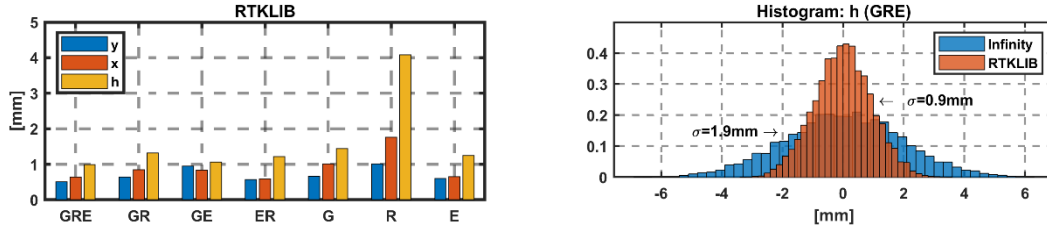


Figure 3: Left: STD of the no motion time series processed with different combinations of satellite systems for RTKLIB. Right: Histogram of height component for RTKLIB and Infinity (GRE)

Based on these results, GRE is used in the ongoing data analysis. By transforming the no motion time series with an FFT into the frequency domain, it can be seen, that noise is equally distributed over all frequencies, so-called white noise, for all three coordinates (y,x,h), with different amplitudes for each of them, see Figure 4. As already discussed before, the height component shows higher amplitudes as y and x, but there is also a difference in amplitude recognizable for y and x, where the East-West component y shows less noise. This can be explained by less satellite coverage in the north at the northern hemisphere, the so-called north hole.

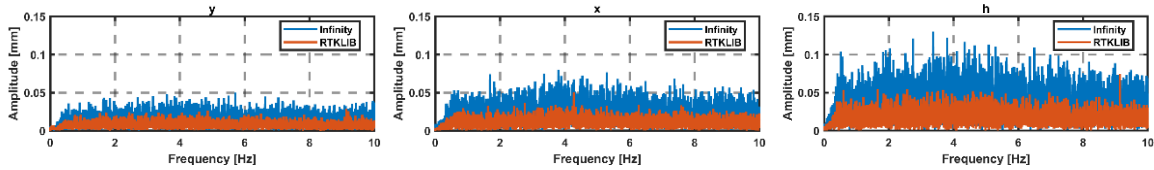


Figure 4: FFT over the no motion part of 7.5 minutes for all three coordinates y (left), x (middle), h (right)

To answer the question if the reference station has also to be operated at the same high measurement rate as the rover, the raw 20Hz reference station data was reduced to 1s and 5s data rate with GFZRNx [10], which are common data rates at reference station networks for network RTK. The data rate of the reference has no influence on the time resolution of the resulting coordinates, which stays at the data rate of the rover. Figure 5 shows, that artefacts in the frequency domain occur, with amplitudes up to 10 times the noise, if the data rate at the reference station is less than the data rate at the rover.

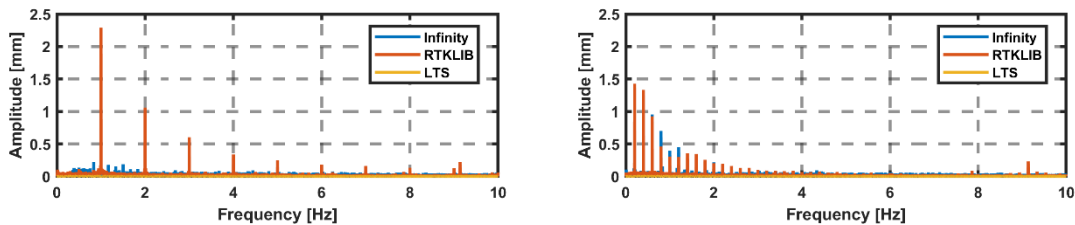


Figure 5: Frequency spectrum with reduced data rate at the reference station (1Hz/1s (left), 0.2Hz/5s (right))

Those artefacts occur at the reference data rate and multiples of it. This is important to keep in mind, and to use a local reference station with an appropriate data rate, if your closest reference station network station does not provide the necessary data rate.

Due to the fact that the shaking table was able to move and it was exposed to wind, the data collection of no motion was repeated for one day with two Leica GR30 receivers, as rover and reference on stable pillars at the rooftop laboratory to further analyse the noise behaviour in the frequency domain over a changing window length. The data was processed in RTKLIB in the same way as the other time series.

Having a closer look at the maximum amplitude of the 3 coordinates, over one hour, for time windows from 1s up to 1h, a clear decrease of the noise amplitude can be seen over time, especially in the first few seconds where a significant drop can be seen from more than 1 mm down to a few hundredths of a millimetre, see Figure 6. Therefore, depending on the amplitude that should be identified, the data length/ (= FFT windows length), has to be chosen accordingly.

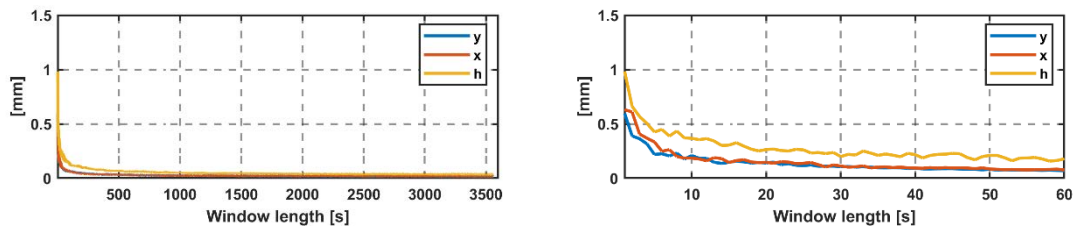


Figure 6: Decrease of maximum amplitude in the noise frequency spectrum over different recording length: Time window length up to one hour (left), zoom in to the first minute (right)

2.2 Sweep and frequency - amplitude combination

For the frequency sweep the shaker was operated from 10Hz to 0.5Hz in 2 minutes with amplitudes below 15mm at both setups, horizontal and vertical. The vertical results were already published in Schönberger et al. [11] therefore only horizontal results are shown here. To introduce time to the FFT a STFT with a window size of 5 seconds was applied to achieve a suitable temporal and frequency resolution and an acceptable noise amplitude. The results for the frequency sweep in the frequency domain are shown in Figure 7.

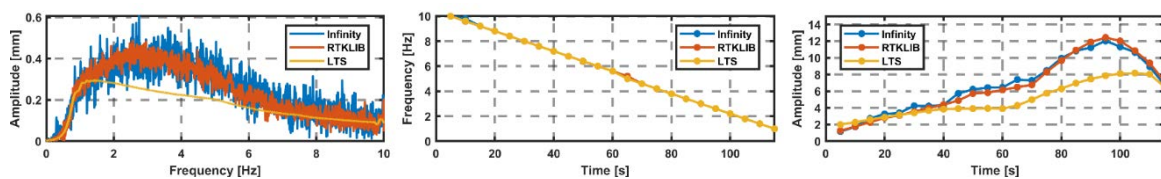


Figure 7: Results of the frequency sweep in the frequency domain, for the whole time (left) and with a STFT with a window length of 5s: Frequency over time (middle) and Amplitude over time (right)

For the frequency amplitude combination, the shaking table was operated in different amplitude steps at a single frequency for 50 seconds over chosen frequencies. A few combinations are shown in Figure 8. The smallest amplitude, that could be recorded in this experiment was $\sim 0.5\text{mm}$ at 3Hz in horizontal direction.

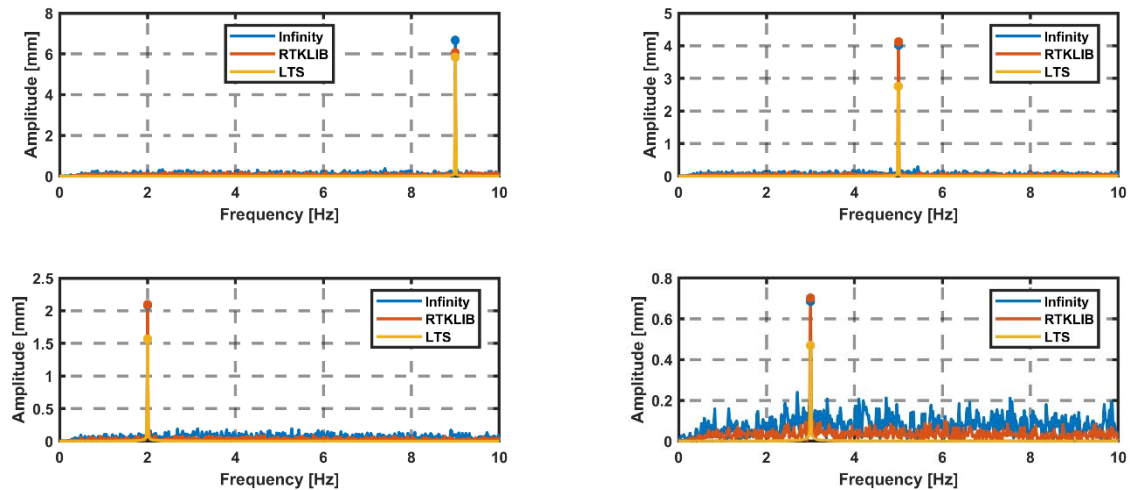


Figure 8: Results of the frequency- amplitude combinations in the frequency domain for frequencies of 2Hz, 3Hz, 5Hz and 9Hz and amplitudes between 0.5mm and 6mm.

The additional results from the shaking table experiment in horizontal direction confirm the conclusion already drawn for the vertical setup. It can be said, that the identification of eigenfrequencies succeeds, but the corresponding amplitudes deviate from the reference measurements with the LTS. Furthermore, the amplitudes calculated with different GNSS software packages differ, although the same raw data is used.

3 FIELD TEST – KÖLNBREINSPERRE

Verbund is one of the largest producers of climate friendly and renewable electricity from hydropower in Europe and generates its electricity on all of the larger rivers in Austria as well as in highly efficient pumped storage power plants like the Kölnbreinsperre in Carinthia.

The Kölnbreinsperre is the highest water dam in Austria and one of the highest arch dams in Europe, with a double curved shape and a maximum crown height of 200m. The crest length is 626m and the additional supporting arch on the downstream side has a height of 70m. The storage volume of the reservoir is 200 million m³.

It is amongst the best monitored civil structures in Austria with a comprehensive surveillance by automatic sensors and regular manual measurements and visual inspections by company staff on site. In general, the monitoring is operated and controlled automatically up to an interval of minutes. The monitoring system consists of approx. 3000 highly sensitive measuring devices, e.g.: hanging and floating plumbs, acceleration sensors etc.

Additionally, geodetic observations are carried out with tachymetry and levelling, in bigger intervals. Monitoring via GNSS is not used at the Kölnbreinsperre so far.

One aim of placing GNSS sensors at Kölnbreinsperre for two 1-month campaigns, one in spring and one in autumn, is to combine static and dynamic monitoring with GNSS sensors on a real infrastructure to test the operation ability for a longer time period. Additionally, the campaign was designed to determine what quality GNSS measurements can deliver for monitoring the Kölnbreinsperre, especially in the flank areas, as these areas are underrepresented in the conventional geodetic measurements.

3.1 Preparation

The preparation of a measurement campaign is crucial to its success, especially for long campaigns in remote areas. Next to the sensor selection and the sensor placement, additional topics, like stable electricity supply and data communication have to be addressed beforehand. A stable electrical power supply was provided by Verbund, but there was no possibility to use ethernet or a mobile network at the sensor locations. For the sensor selection a data rate of 20Hz and the ability to receive GPS, GLONASS and Galileo signals was mandatory. With the selected Leica GR30 receivers, placed as a reference and at the four single sites, the recorded data could be compressed and stored in a Leica MDB format, so that the data of a whole month fit on a 32GB SD card per receiver. For the Novatel PwrPak7 with a dual antenna, placed in the centre of the dam, the recorded LOG files were stored on a 128GB USB Stick, which had to be replaced once. The size of all decompressed and into RINEX 3 converted data, resulted in ~1TB per campaign.

In the run-up to the GNSS measurements on the Kölnbreinsperre, the exact locations of the GNSS antennas, and receivers were evaluated and determined, Figure 9. Locations in the flank areas (M1 and M5) were deliberately chosen to provoke scenarios with large obstructions and high multipath. The two lateral sensors are also necessary for the static observation, as they represent the entire structure together with the three central stations.

The GNSS stations M2, M3 and M4 are located in the same vertical blocks as other relevant permanent measuring devices of the dam, in particular, the hanging plumbs (in further extension floating plumbs) and the acceleration sensors. In the middle of the dam (M3), where the largest displacements were expected, a second antenna (D3) was mounted on the air side, to also record the displacements of the dam at the side of the air. As a reference station a measurement pillar, close to the water dam (baseline lengths < 750m) was used. A photo of the stations M1 and M5 is shown in Figure 10.

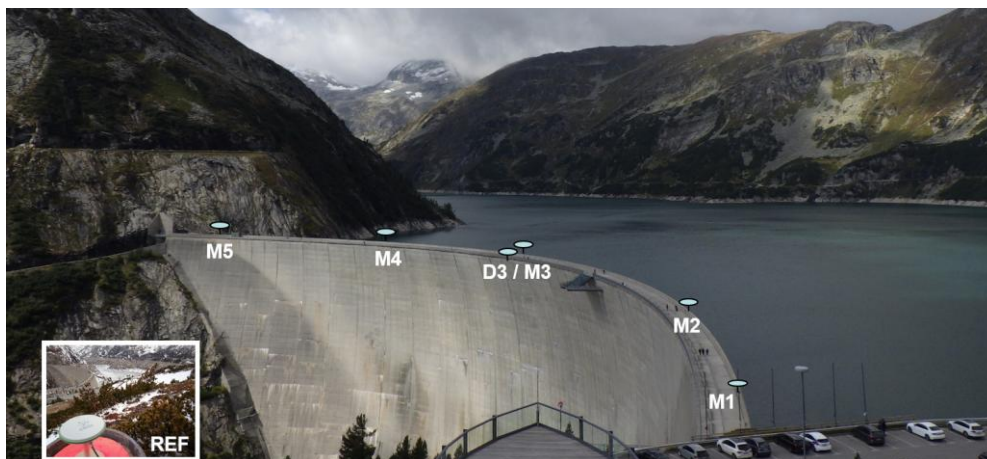


Figure 9: Sensor placement at Kölnbreinsperre



Figure 10: Photo of station M5(left) and M1(right) after the setup in April 2022

3.2 Static Data Analysis

For the static data analysis, GNSS data were processed in one-hour blocks leading to one 3D coordinate per hour for each point. Figure 11 (left), shows the scaled deformation between the first and the last measurement, which is mainly due to a rising water level over the summer. In April the water level was at a low point, whereas in October the dam was fully filled. The maximum recorded displacement was close to 100mm at the centre of the dam, compared to the movement at the abutments, with a maximum movement of less than 10mm, which is one tenth of the movement in the centre, Figure 11 (right). The GNSS derived displacement in the centre of the dam fits well to the plumb line data. The processing of the other plumb lines is currently ongoing.

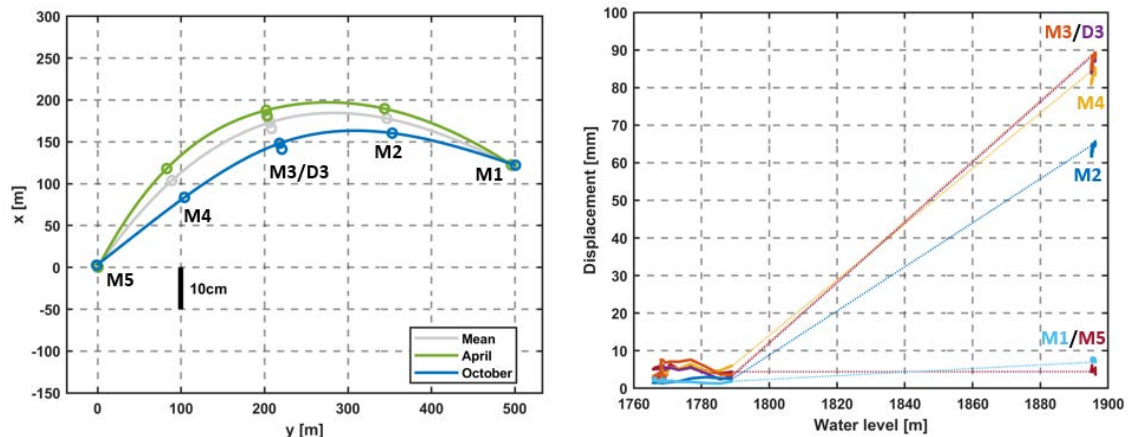


Figure 11: Left: First epoch in April (green), last epoch in October (blue) and mean values (grey) for all stations. The deformation is scaled (scaling bar); Right: Displacement as a function of water level change

It can be seen, that the main component of the displacement happens in radial direction (in direction to the air), especially for M3, with nearly no displacement in tangential direction, Figure 12. At the two stations M2 and M4, there is also an nearly equal part of displacement in tangential direction and in the direction to the abutments of ~40mm.

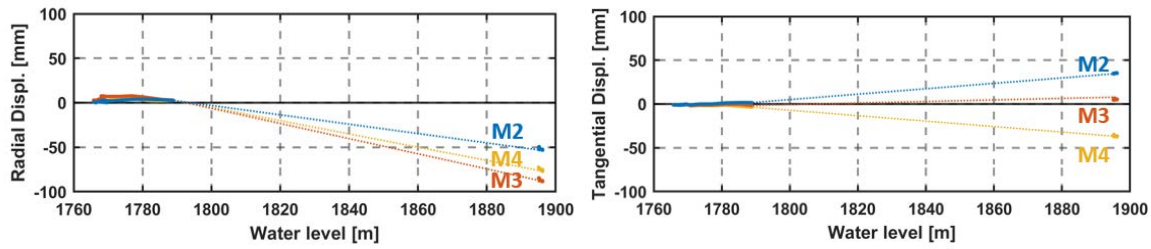


Figure 12: Daily radial (left) and tangential (right) displacement of the dam as a function of water level for the two measurement campaigns.

3.3 Benefit of Multi-constellation GNSS

Especially at antenna locations with obstacles to the sky an improvement of number of satellites, Dilution of Precision (DOP), precision and fixed solutions is expected, by using more satellite systems than only GPS. To evaluate the improvement of the European Galileo system, this section shows a comparison of data processing using only GPS (G), GPS and Galileo (GE), and GPS, GLONASS and Galileo (GRE) combined, for a station with good view to the sky (M1), and a station which is located close to the nearby mountain slope (M5), Figure 10, during for both measurement campaigns in spring and in autumn.

To calculate a meaningful standard deviation the movement of the dam (moving average of 24h) was subtracted of the time series. Figure 13 shows the standard deviation for the different satellite system combinations for each coordinate. For the station M5 a huge overall improvement of around 25% can be achieved with the addition of Galileo signals and around 35% with the addition of Galileo and GLONASS signals, with the largest improvements in x-direction.

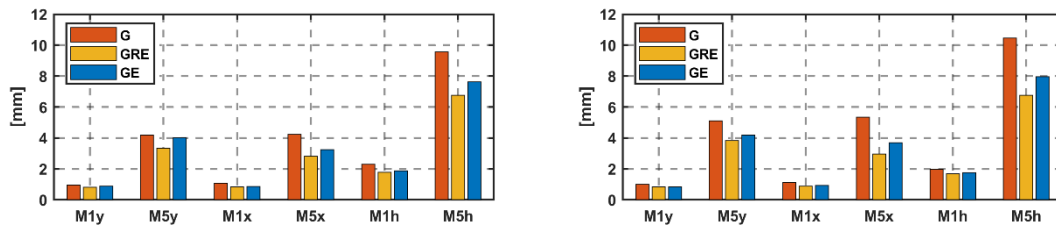


Figure 13: Standard deviation of the static time series of the station M1 and M5 for all 3 coordinates, calculated with only GPS (G), GPS + GLONASS + Galileo (GRE) and GPS + GALILEO signals (GE). Measurement campaign in spring (left) and Measurement campaign in autumn (right)

Also, an improvement in the geometric DOP (GDOP) value, over one day for station M5, is clearly seen, with a maximum value below 8 for the additional use of Galileo signals, and below 5 for GPS, GLONASS and Galileo, whereas the GDOP for only GPS signals is up to 24, Figure 14, left. The GDOP depends also on the number of satellites, which varies from 4 to 8 satellites for each satellite system to more than 10 for both GPS and Galileo, and up to 19 with GPS, GLONASS and Galileo Figure 14, right.

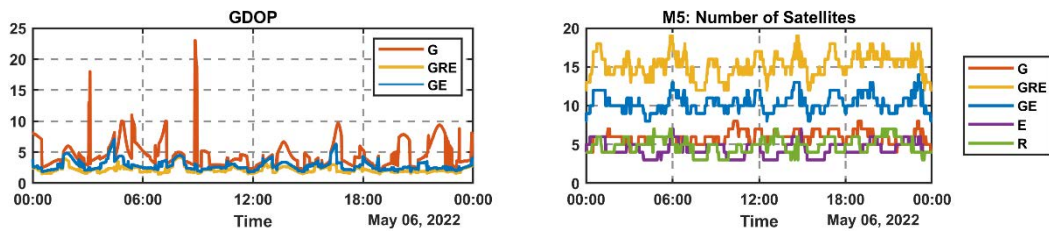


Figure 14: GDOP variation (left) and number of satellites(right) for station M5

For dynamic data analysis the percentage of fixed solutions is important. Therefore, the GNSS data was calculated in kinematic mode with 20Hz data rate. Figure 15 (spring) and Figure 16 (autumn) show the percentage for each hour. 100% would be the best value and with GPS and Galileo signals the percentage of fixed solution per hour is at a minimum of 70% whereas it is only 9% with only GPS. Over the whole campaign ~99% of data result in a fixed solution for GPS and Galileo and ~96% for only GPS. The difference of 3% results in nearly 2 minutes per hour, or 5 hours per week. With the additional use of GLONASS signals a decrease of fixed solutions is observable, with even less percent than only GPS. Therefore, GPS and Galileo signals are used for dynamic processing.

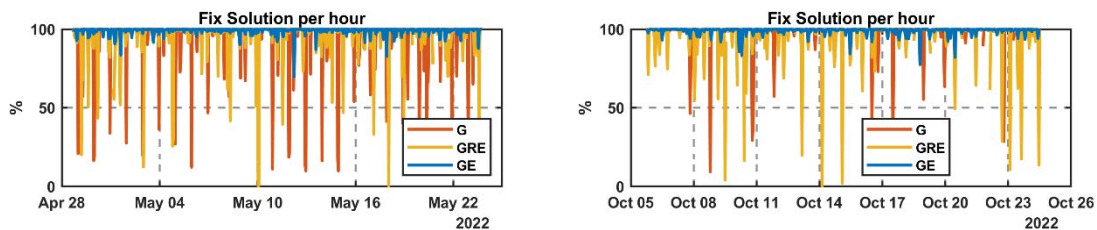


Figure 15: Percentage of fixed solution per hour for GNSS data in kinematic mode for the first campaign in May (left) and the second campaign in October (right)

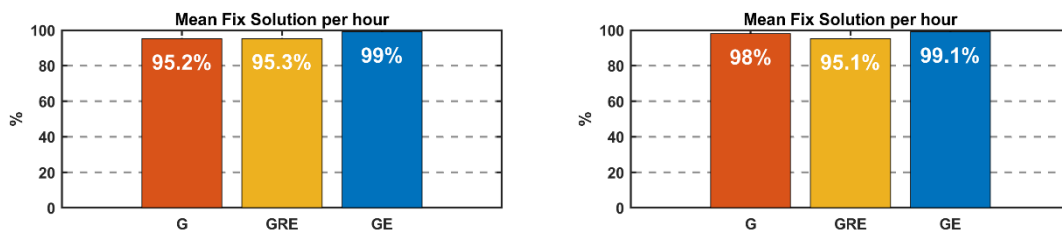


Figure 16: Percentage of fixed solution for GNSS data in kinematic mode for the first campaign in May (left) and the second campaign in October (right)

3.4 Dynamic Data Analysis

No major dynamic events were recorded during the two measurement campaigns at the GNSS receivers. This is verified by acceleration sensors operated by Verbund.

On the last day of measurements, waves occurred on the reservoir arriving from Northwest. Bigger waves have frequencies between 0.1Hz and 10Hz [12], so the question occurred, if they are visible in the GNSS data. The station M4 was chosen, due to its orientation, and a STFT, with a window length of 1 hour, over the radial component of all data in October was calculated, Figure 17 left. A view brighter spots (marked in red), are visible within the

frequency range of 0.7Hz to 1.3Hz and amplitudes smaller than 0.04mm. Taking the maximum amplitude in that frequency range and plot it over the windspeed from Northwest, a clear correlation is recognizable. Therefore, the waves on the reservoir are visible in our GNSS data, although their amplitudes are very low.

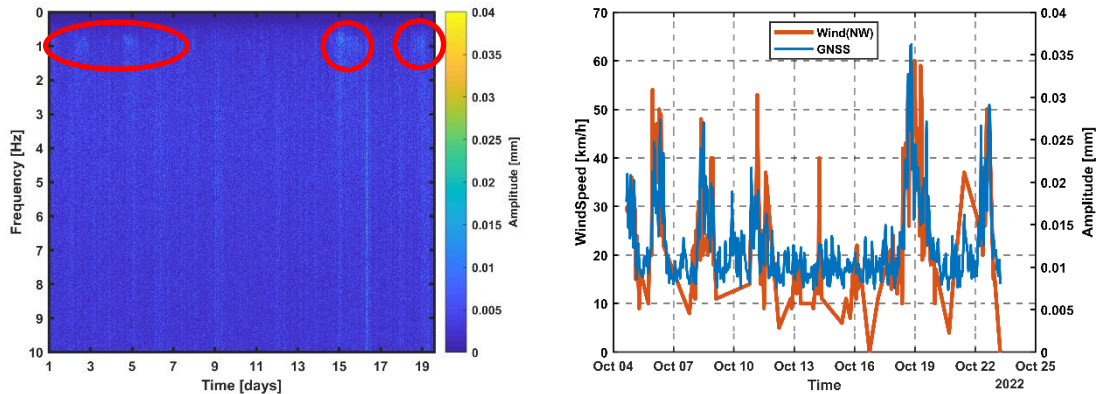


Figure 17: Left: STFT (window length of 1h) over the campaign in October for station M4 in radial direction. Right: Maximal amplitude in the frequency range from 0.7Hz to 1.3Hz and wind data from Northwest.

4 CONCLUSIONS

This paper shows the suitability of GNSS receivers in SHM for monitoring the static displacement and the dynamic response of an object with one sensor type. Therefore, the data collection was carried out with GNSS receivers with a data rate of 20Hz and the three satellite systems: GPS, GLONASS and Galileo.

For the experiments in the laboratory, it can be concluded, that it is very important to provide the same data rate at the rover and the reference receiver to avoid artefacts in the frequency spectrum. Furthermore, the noise behaves like white noise in the frequency spectrum, with decreasing amplitudes, the longer signal length lasts. With a frequency sweep and frequency amplitude combinations, the identification of frequencies and their corresponding amplitude was tested. The identification of frequencies succeeded, but there are differences in the amplitudes, between the reference measurements and the results from different GNSS software packages.

To test the results on a real object, 6 GNSS receivers were mounted on the highest water dam in Austria, Kölnbreinsperre for two 1-month long campaigns. In the static time series, a displacement of $\sim 100\text{mm}$ was recorded due to the water level rise. This data was compared to plumb data from the operator, Verbund.

For the station very close to the nearby slope, an improvement in precision could be achieved with the additional use of Galileo and GLONASS to GPS. For the dynamic data processing a high value in fixed solutions is necessary. This value could be improved with Galileo signals but got even worse with the addition of GLONASS. Therefore, it is suggested to record GPS, GLONASS and Galileo signals on the rover, and use that data for static data processing, but only use GPS and Galileo for dynamic data processing. Although no major dynamic events occurred at the water dam during the observation period, first result indicate that small scale vibrations of the crown due to waves may be identifiable by dynamic GNSS measurements.

ACKNOWLEDGEMENTS

We acknowledge the funding of this innovative project by the Austrian Research Promotion Agency (FFG) within the Austrian Space Applications Programme (ASAP PNO: 888310).

REFERENCES

- [1] Im, S. B., Hurlebaus, S., & Kang, Y. J. (2013). Summary review of GPS technology for structural health monitoring. *Journal of Structural Engineering*, 139(10), 1653-1664.
- [2] Moschas, F., & Stiros, S. (2011). Measurement of the dynamic displacements and of the modal frequencies of a shortspan pedestrian bridge using GPS and an accelerometer. *Engineering structures*, 33(1), 10-17.
- [3] Górski, P. (2017). Dynamic characteristic of tall industrial chimney estimated from GPS measurement and frequency spe decomposition. *Engineering Structures*, 148, 277-292.
- [4] Yi, J., Zhang, J. W., & Li, Q. S. (2013). Dynamic characteristics and wind-induced responses of a super-tall building during typhoons. *Journal of Wind Engineering and Industrial Aerodynamics*, 121, 116-130.
- [5] Shen, N., Chen, L., Liu, J., Wang, L., Tao, T., Wu, D., & Chen, R. (2019). A review of global navigation satellite system (GNSS)-based dynamic monitoring technologies for structural health monitoring. *Remote Sensing*, 11(9), 1001.
- [6] Shannon, C. E. (1949). Communication in the presence of noise. *Proceedings of the IRE*, 37(1), 10-21.
- [7] Takasu, T. (2011). RTKLIB: An open source program package for GNSS positioning.
- [8] Paziewski, J., Sieradzki, R., & Baryla, R. (2019). Detection of structural vibration with high-rate precise point positioning: case study results based on 100 Hz multi-GNSS observables and shake-table simulation. *Sensors*, 19(22), 4832.
- [9] Micro Epsilon (2019) Operating Instructions optoNCDT 1700, 112 p.
- [10] Nischan, T. (2016): GFZRNX - RINEX GNSS Data Conversion and Manipulation Toolbox. GFZ Data Services. <http://dx.doi.org/10.5880/GFZ.1.1.2016.002>
- [11] Schönberger, C., Lienhart, W., & Moser, T. (2022). Dynamic monitoring of civil infrastructures with geodetic sensors. In 5th Joint International Symposium on Deformation Monitoring: JISDM 2022, pp. 537-543. <http://dx.doi.org/10.4995/JISDM2022.2022.16057>.
- [12] Munk, W. H. (1951). Origin and generation of waves. Scripps Institution of Oceanography La Jolla Calif.